

A discriminating probe of gravity at cosmological scales

Pengjie Zhang,^{1,2} Michele Liguori,³ Rachel Bean,⁴ and Scott Dodelson^{5,6}

¹Shanghai Astronomical Observatory, Chinese Academy of Science, 80 Nandan Road, Shanghai, China, 200030

²Joint Institute for Galaxy and Cosmology (JOINGC) of SHAO and USTC

³Department of Applied Mathematics and Theoretical Physics,
Centre for Mathematical Sciences, University of Cambridge,
Wilberforce Road, Cambridge, CB3 0WA, United Kingdom

⁴Department of Astronomy, Cornell University, Ithaca, NY 14853

⁵Center for Particle Astrophysics, Fermi National Accelerator Laboratory, Batavia, IL 60510-0500

⁶Department of Astronomy & Astrophysics, The University of Chicago, Chicago, IL 60637-1433*

The standard cosmological model is based on general relativity and includes dark matter and dark energy. An important prediction of this model is a fixed relationship between the gravitational potentials responsible for gravitational lensing and the matter overdensity. Alternative theories of gravity often make different predictions for this relationship. We propose a set of measurements which can test the lensing/matter relationship, thereby distinguishing between dark energy/matter models and models in which gravity differs from general relativity. Planned optical, infrared and radio galaxy and lensing surveys will be able to measure E_G , an observational quantity whose expectation value is equal to the ratio of the Laplacian of the Newtonian potentials to the peculiar velocity divergence, to percent accuracy. We show that this will easily separate alternatives such as Λ CDM, DGP, TeVeS and $f(R)$ gravity.

PACS numbers:

Introduction.— Predictions based on general relativity plus the Standard Model of particle physics are at odds with a variety of independent astronomical observations on galactic and cosmological scales. This failure has led to modifications in particle physics. By introducing dark matter and dark energy, cosmologists have been able to account for a wide range of observations, from the overall expansion of the universe to the large scale structure of the early and late universe [1]. Alternatively, attempts have been made to modify general relativity at galactic [2] or cosmological scales [3, 4]. A fundamental question then arises: *Can the two sets of modifications be distinguished from one another?*

The answer is “No” if only the zero order expansion of the universe is considered. By allowing the dark energy equation of state w_{DE} to be a free function, the expansion history $H(z)$ produced by any modified gravity can be mimicked exactly. Fortunately, structure formation in modified gravities in general differs [5, 6, 7, 8, 9, 10, 11, 12, 13, 14, 15, 16] from that in general relativity. The difference we focus on here is the relationship between gravitational potentials responsible for gravitational lensing and the matter overdensity. Lensing is sensitive to $\nabla^2(\phi - \psi)$ along the line of sight where ϕ and ψ are the two potentials in the perturbed Friedman-Robertson-Walker metric: $ds^2 = (1 + 2\psi)dt^2 - a^2(1 + 2\phi)dx^2$ and a is the scale factor. In standard general relativity (GR), in the absence of anisotropic stresses, $\phi = -\psi$, so lensing is sensitive to

$\nabla^2\phi$. The Poisson equation algebraically relates $\nabla^2\phi$ to the fractional overdensity δ , so lensing is essentially determined by δ along the line of sight. This is a prediction of the standard, GR-based theory that is generally not obeyed by alternate theories of gravity.

Testing this prediction is non-trivial. Astronomers often use the galaxy overdensity as a probe of the underlying matter overdensity, but the two are not exactly equal. Here we propose a test of this prediction which is relatively insensitive to the problem of galaxy bias. The basic idea is simple:

- Extract the matter overdensity at a given redshift by measuring the velocity field. Matter conservation relates velocities to the overdensities. The measurement of the velocity field can be accomplished by studying the anisotropy of the galaxy power spectrum in redshift space.
- Extract the lensing signal at this redshift by cross-correlating these galaxies and lensing maps reconstructed from background galaxies.

More quantitatively, the galaxy-velocity cross power spectrum $P_{g\theta} \equiv -\langle\delta_g(\mathbf{k})\theta(-\mathbf{k})\rangle$ can be inferred from redshift distortions in a galaxy distribution. Here, $\theta \equiv \nabla \cdot \mathbf{v}/H(z)$ and \mathbf{v} is the comoving peculiar velocity. In the linear regime, matter conservation relates θ to δ by $\theta = -\dot{\delta}/H = -\beta\delta$, where $\beta \equiv d \ln D/d \ln a$ and D is the linear density growth factor. So, $P_{g\theta} = \beta P_{g\delta}$, satisfying the first goal above. Cross correlating the same galaxies with lensing maps constructed from galaxies at higher redshifts, $P_{\nabla^2(\phi-\psi)g}$ can be measured. The ratio of these two cross-spectra therefore is a direct probe

*Electronic address: pjzhang@shao.ac.cn

of $\nabla^2(\phi - \psi)/(\beta\delta)$. It does not depend on galaxy bias or on the initial matter fluctuations, at least in the linear regime. Modifications in gravity will in general leave signatures in either β and/or the Poisson equation.

Galaxy-Velocity Cross-correlation.— A galaxy's peculiar motion shifts its apparent radial position from x_z to $x_z^s = x_z + v_z/H(z)$ in redshift space, where v_z is the comoving radial peculiar velocity. The coherent velocity component changes the galaxy number overdensity from δ_g to $\delta_g^s \simeq \delta_g - \nabla_z v_z/H(z)$. Galaxy random motions mix different scales and damps the power spectrum on small scales. The redshift space galaxy power spectrum therefore has the general form ([17] and references therein)

$$P_g^s(\mathbf{k}) = [P_g(k) + 2u^2 P_{g\theta}(k) + u^4 P_\theta(k)] F\left(\frac{k^2 u^2 \sigma_v^2}{H^2(z)}\right) \quad (1)$$

where $u = k_{\parallel}/k$ is the cosine of the angle of the \mathbf{k} vector with respect to radial direction; P_g , $P_{g\theta}$, P_θ are the real space galaxy power spectra of galaxies, galaxy- θ and θ , respectively; σ_v is the 1D velocity dispersion; and $F(x)$ is a smoothing function, normalized to unity at $x = 0$, determined by the velocity probability distribution. This simple formula has passed tests in simulations on scales where $\delta \lesssim 1$ [17]. The derivation of Eq. (1) is quite general, so it should be applicable even when gravity is modified.

The distinctive dependence of P_g^s on u allows for simultaneous determination of P_g , $P_{g\theta}$ and P_θ [18]. The parameters we want to determine are the band powers of $P_{g\theta}(k)$ ¹ defined such that $P(k) = P_\alpha$ if $k_\alpha \leq k < k_{\alpha+1}$, where $k_1 < k_2 < \dots < k_\alpha < \dots$. We denote $P_\alpha^{(1)}$ as the band power of $P_{g\theta}$. For a \mathbf{k}_i in each k bin, we have a measurement of P_g^s , which we denote as P_i . The unbiased minimum variance estimator of $P_\alpha^{(1)}$ is

¹ Distance D and H are required to translate the observed galaxy angular and redshift separation to \mathbf{k} . In general, errors in D and H measurements cause both horizontal and vertical shifts in the E_G plot. Both D and H will be measured by methods like type Ia supernovae and baryon acoustic oscillations with 1% accuracy, much smaller than the k bin size adopted, so the horizontal shift is negligible. Errors in D show up in both $P_{g\theta}$ and the $C_{\kappa g} \rightarrow P_{\nabla^2(\psi-\phi)_g}$ inversion through $l = kD$ and thus largely cancel in evaluating E_G . Errors in $H(z)$ only show up in $P_{g\theta}$ measurement and thus cause a net shift in the value of E_G . For 1% error in H , the fractional error in E_G is $\leq (n_{\text{eff}} + 3)1\% \leq 3\%$. Here, n_{eff} is the effective power index of the corresponding power spectra. For the fiducial Λ CDM cosmology, it is negative in relevant k range. Thus errors induced by uncertainties in $D(z)$ and $H(z)$ measurement will be sub-dominant, except for SKA, which requires better control over systematic errors in D and H measurement. For simplicity, we neglect this potential error source. Measuring $P_{g\theta}$ also requires to marginalize over σ_v . However, in the linear regime $k \lesssim 0.2h/\text{Mpc}$, $k^2 \sigma_v^2/H^2 \ll 1$ and $F(k^2 u^2 \sigma_v^2/H^2) \simeq 1$, for typical value $\sigma_v \sim 300$ km/s. Thus the exact value of σ_v is not required for our analysis. Without loss of generality, we adopt $\sigma_v = 300$ km/s.

$\hat{P} = \sum W_i P_i$, where $W_i = \frac{F_i}{2\sigma_i^2}(\lambda_1 + \lambda_2 u_i^2 + \lambda_3 u_i^4)$. Here, $F_i \equiv F(k u_i \sigma_v/H)$, σ_i^2 is the variance of P_i and the three Lagrange multipliers λ_α ($\alpha = 1, 2, 3$) is determined by

$$\lambda = (0, \frac{1}{2}, 0) \cdot \mathbf{A}^{-1}; \quad A_{mn} = \sum_i u_i^{2(m+n-2)} \frac{F_i^2}{2\sigma_i^2}. \quad (2)$$

Galaxy-galaxy lensing.— Weak lensing is sensitive to the convergence κ , the projected gravitational potential along the line of sight:

$$\kappa = \frac{1}{2} \int_0^{\chi_s} \nabla^2(\psi - \phi) W(\chi, \chi_s) d\chi. \quad (3)$$

Here, W is the lensing kernel. For a flat universe, χ, χ_s are the comoving angular diameter distance to the lens and source, respectively. Eq. 3 is a pure geometric result and can be applied to any modified gravity models where photons follow null geodesics.

A standard method to recover the lens redshift information is by the lensing-galaxy cross correlation. For galaxies in the redshift range $[z_1, z_2]$, the resulting cross correlation power spectrum under the Limber's approximation is

$$\begin{aligned} C_{\kappa g}(l) &= \left(4 \int_{\chi_1}^{\chi_2} n_g(\chi) d\chi\right)^{-1} \\ &\times \int_{\chi_1}^{\chi_2} W(\chi, \chi_s) n_g(\chi) P_{\nabla^2(\psi-\phi)_g}\left(\frac{l}{\chi}, z\right) \chi^{-2} d\chi \\ &\simeq \frac{W(\bar{\chi}, \chi_s)}{4l\Delta\chi} \int_{l/\chi_2}^{l/\chi_1} P_{\nabla^2(\psi-\phi)_g}(k, \bar{z}) dk \\ &= \sum_\alpha f_\alpha(l) P_\alpha^{(2)}. \end{aligned} \quad (4)$$

Here, $\chi_{1,2}$ are the comoving angular diameter distance to redshift $z_{1,2}$ and $\bar{\chi}$ is the mean distance. The band power $P_\alpha^{(2)}$ of $P_{\nabla^2(\psi-\phi)_g}$ is defined at the same k range as $P_\alpha^{(1)}$. In practice, we measure the band power $C_{\kappa g}(l, \Delta l)$, centered at l with band width Δl . The weighting $f_\alpha(l, \Delta l)$ is defined correspondingly. For each l , only a fraction of α having $f_\alpha(l, \Delta l) \neq 0$ contribute.

A discriminating probe of gravity.— With the above measurements, one can construct an estimator

$$\hat{E}_G = \frac{C_{\kappa g}(l, \Delta l)}{3H_0^2 a^{-1} \sum_\alpha f_\alpha(l, \Delta l) P_\alpha^{(1)}}, \quad (5)$$

whose expectation value is

$$\langle \hat{E}_G \rangle = \left[\frac{\nabla^2(\psi - \phi)}{-3H_0^2 a^{-1} \theta} \right]_{k=\frac{l}{\bar{\chi}}, \bar{z}} = \left[\frac{\nabla^2(\psi - \phi)}{3H_0^2 a^{-1} \beta \delta} \right]_{k=\frac{l}{\bar{\chi}}, \bar{z}} \equiv E_G. \quad (6)$$

The fractional error on \hat{E}_G is

$$\frac{\langle \Delta E_G^2 \rangle}{E_G^2} \simeq \frac{\Delta C^2}{C_{\kappa g}^2} + \frac{\sum_\alpha f_\alpha^2 \langle (\delta P_\alpha^{(1)})^2 \rangle}{(\sum_\alpha f_\alpha P_\alpha^{(1)})^2}, \quad (7)$$

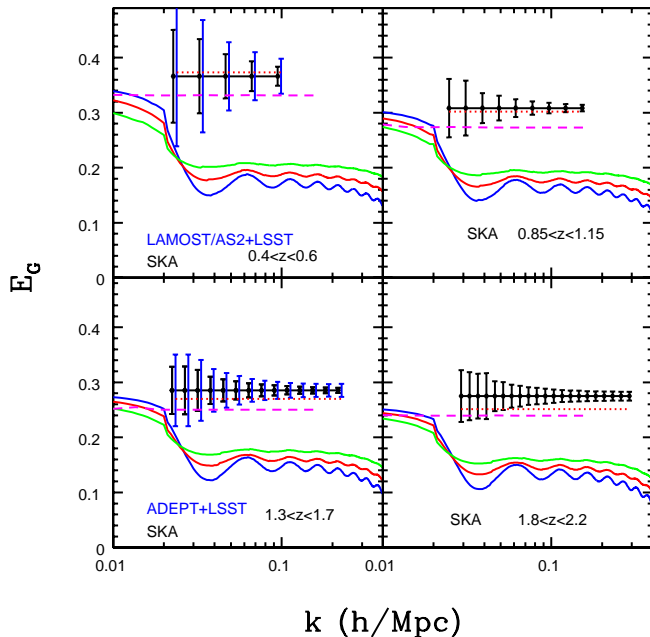


FIG. 1: E_G as a smoking gun of gravity. Error estimation is based on Λ CDM and error bars are centered on the Λ CDM prediction (black solid straight line). We only show those k modes well in the linear regime. For clarity, we shift the error bars of LAMOST/AS2+LSST and ADEPT+LSST slightly rightward. Irregularities in the error-bars are caused by irregularities in the available discrete k modes of redshift distortion. Dotted lines are the results of a flat DGP model with $\Omega_0 = 0.2$. Dashed lines are for $f(R) = -\lambda_1 H_0^2 \exp(-R/\lambda_2 H_0^2)$ with $\lambda_2 = 100$. Differences in expansion histories of these models are of percent level at $z < 2$ and are not the main cause of differences in E_G . Solid lines with wiggles are for TeVeS with $K_B = 0.08, 0.09, 0.1$, where the lines with most significant wiggles have $K_B = 0.1$.

where $\Delta C^2 = [C_{\kappa g}^2 + (C_\kappa + C_\kappa^N)(C_g + C_g^N)]/(2l\Delta l f_{\text{sky}})$. Here, C_κ , C_κ^N , C_g , C_g^N are the power spectra of weak lensing convergence, weak lensing shot noise, galaxy and galaxy shot noise, respectively, and f_{sky} is the fractional sky coverage. Errors on E_G at any two adjacent bins are correlated, since they always share some same k modes. However, by requiring $l_\alpha/\chi_1 = l_{\alpha+1}/\chi_2$, where $l_1 < l_2 < \dots < l_\alpha < \dots$ and $k_\alpha = l_\alpha/\chi_2$, E_G measurement at each l bin only involves two k bins and thus only errors in adjacent bins are correlated.

We choose ongoing/proposed spectroscopic surveys LAMOST, AS2, ADEPT and SKA as targets of redshift distortion measurements, and LSST and SKA as targets of lensing map reconstruction. SKA lensing maps can be constructed through cosmic magnification utilizing its unique flux dependence, with S/N comparable to that of LSST through cosmic shear [19]. Survey specifications are summarized in TABLE I. The fiducial cosmology adopted is the Λ CDM cosmology, with the WMAP best

TABLE I: Summary of target surveys.

	redshift	deg ²	N_{gal}	band	operation
LAMOST ^a	$z < 0.8$	10,000	$\sim 10^6$	optical	2008
AS2 ^b	$z < 0.8$	10,000	$\sim 10^6$	optical	≥ 2009
ADEPT ^c	$1 < z < 2$	28,600	$\sim 10^8$	infrared	≥ 2009
SKA ^d	$z \lesssim 5$	22,000	$\sim 10^9$	radio	2020
LSST ^e	$z \lesssim 3.5$	10,000	$\sim 10^9$	optical	2012

^a<http://www.lamost.org/en/>

^bPrivate communication with Daniel Eisenstein

^chttp://www7.nationalacademies.org/ssb/BE_Nov_2006_bennett.pdf

^d<http://www.skatelescope.org/>

^e<http://www.lsst.org>

fit parameters $\Omega_0 = 0.26, \Omega_\Lambda = 1 - \Omega_0, h = 0.72, \sigma_8 = 0.77$ and $n_s = 1$. The result is shown in figure 1. In general, at $k < 0.1 h/\text{Mpc}$, cosmic variance in $C_{\kappa g}$ and $P_{g\theta}$ measurements dominates the E_G error budget, resulting in decreasing error-bars toward larger k . This makes f_{sky} and the lensing source redshifts the two most relevant survey parameters for E_G error estimation. Since systematic errors in LSST photometric redshifts can be controlled to better than 1%, errors in E_G measurements of LAMOST/AS2+LSST and ADEPT+LSST caused by source redshift uncertainties are sub-dominant.

We restrict our discussion to sub-horizon scale perturbations and express equations hereafter in the Fourier form. Four independent linear equations are required to solve for four perturbation variables δ , θ , ψ and ϕ . The mass-energy conservation provides two: $\delta + H\theta = 0$ and $\dot{H}\theta + 2H^2\theta - k^2\psi/a^2 = 0$. For at least Λ CDM, quintessence-CDM, DGP and $f(R)$ gravity, the other two takes the general form

$$\begin{aligned} \phi &= -\eta(k, a)\psi, \\ k^2(\phi - \psi) &= 3H_0^2\Omega_0 a^{-1}\delta\tilde{G}_{\text{eff}}(k, a). \end{aligned} \quad (8)$$

Here Ω_0 is the cosmological matter density in unit of the critical density $\rho_c \equiv 3H_0^2/8\pi G$. Refer to [14, 15, 16] for other ways of parameterizations. MOND has extra scalar and vector perturbations and does not follow the general form of Eq. 8 [6, 7].

(1) **Λ CDM:** $\eta = 1$, $\tilde{G}_{\text{eff}} = 1$ and $E_G = \Omega_0/\beta$. Dynamical dark energy will have large-scale fluctuations [20]. Furthermore, it may also have non-negligible anisotropic stress and is thus able to mimic modifications in gravity [21]. But, for models with large sound speed and negligible anisotropic stress, such as quintessence, these are negligible at sub-horizon scales and Eq. 8 still holds.

(2) **Flat DGP:** $\eta = [1 - 1/3\beta_{\text{DGP}}]/[1 + 1/3\beta_{\text{DGP}}]$, $\tilde{G}_{\text{eff}} = 1$ [9] and $E_G = \Omega_0/\beta$, where $\beta_{\text{DGP}} = 1 - 2r_c H(1 + \dot{H}/3H^2) < 0$ and $r_c = H_0/(1 - \Omega_0)$. Ω_0 differs from that of Λ CDM, in order to mimic $H(z)$ of Λ CDM.

(3) **$f(R)$ gravity:** in the sub-horizon limit, $\tilde{G}_{\text{eff}} = (1 + f_R)^{-1}$ [11] and $\eta = 1$ [12], with $f_R \equiv df/dR|_B$ where B denotes the FRW background. This falls naturally out of a conformal transformation of the expression for E_G

in the Einstein frame into the Jordan frame, noting that Einstein frame scalar field fluctuations are negligible on sub-horizon scales [12]. We numerically solve the full perturbation equations in the Einstein frame since it is computationally simpler [12] and then conformally transform to the Jordan frame, which we choose as the physical frame, evaluating β such that $E_G = \Omega_0/(1+f_R)\beta$. In the limit that $f_R \rightarrow 0$, e.g. for $f(R) \sim \lambda_1 H_0^2 \exp(-R/\lambda_2 H_0^2)$ [11] with $\lambda_1 \ll \lambda_2$, the evolution is observationally equivalent to Λ CDM. For modes that entered the horizon prior to matter-radiation equality, as we consider here, β , and therefore E_G , is scale invariant for IR modifications to gravity, with $f_R > 0$.² The scale independence of E_G holds in Λ CDM, Quintessence-CDM and DGP. An observed scale-independent deviation in E_G from Λ CDM could signify a special class of modified gravity, as shown in Fig. 1.

(4) **TeVes/MOND**. Besides the gravitational metric, TeVeS [2] contains a scalar and a vector field. These new fields act as sources for the gravitational potential ϕ in the modified Poisson equation and can change the evolution of cosmological perturbations with respect to standard gravity [6, 7]. We considered a TeVeS model with $\Omega_b = 0.05$, $\Omega_\nu = 0.17$, $\Omega_\Lambda = 0.78$ and we adopted a choice of the TeVeS parameters that produces a significant enhancement of the growth factor. The TeVeS E_G is significantly different from the standard E_G (Fig. 1).³ It exhibits scale dependence with accompanying baryon acoustic wiggles. Both features are due to the vector field fluctuations, which *play a significant role* in structure formation [7]. These fluctuations decrease toward small scales and cause the scale dependency of E_G . We also checked that they affect the final shape of the acoustic oscillations of the other components significantly. As a result, oscillations in ϕ , ψ and δ do not cancel out perfectly in TeVeS when we take the ratio, thus producing the wiggles in E_G .

For the four gravity models investigated, differences in E_G are much larger than observational statistical uncertainties. Planned surveys are promising to detect percent level deviation from GR and should distinguish these modified gravity models unambiguously.

At large scales, gravity is the only force determining the acceleration of galaxies and dark matter particles. So we assumed no galaxy velocity bias. As statistical errors in E_G measurements reach the 1% level (Fig. 1), several systematics, besides the one discussed in footnote 1, may become non-negligible. One is the accuracy of the redshift distortion formula (Eq. 1), which may be problematic for those modes with large u , even at very linear scales [17]. A remedy is to exclude them when extracting $P_{g\theta}$, at the expense of statistical accuracy. As discussed before, accuracy of E_G measurement is dominated by accuracy of $P_{\nabla^2(\psi-\phi)g}$ measurements and is thus less affected. A less severe one is the nonlinear evolution, which becomes non-negligible where the matter power spectrum variance $\Delta_m^2 \gtrsim 0.1$. In general relativity, nonlinear corrections to density and velocity differ (Fig. 12, [22]). A direct consequence is that E_G develops a dependence on the matter power spectrum. Similar effects in modified gravity models are expected. This can be corrected by high order perturbation calculations, which should work well where $\Delta_m^2 \lesssim 0.2$.

We thank R. Caldwell, D. Eisenstein, B. Jain, M. Kunz, J. Ostriker and J.P. Uzan for useful discussions and the anonymous referees for useful suggestions. PJZ is supported by the National Science Foundation of China grant 10533030 and CAS grant KJCX3-SYW-N2. RB's work is supported by the National Science Foundation grants AST-0607018 and PHY-0555216. SD is supported by the US Department of Energy.

² Scales larger than the horizon at matter-radiation equality are suppressed [12] and, if measurable, would have a scale dependent increase in the value of E_G in comparison to the small scale value.

³ To simplify the numerical treatment of the TeVeS perturbations equations while retaining a good qualitative description of all the significant physical effects at the same time, we introduced several approximations. Namely we assumed instantaneous recombination and employed the tight coupling approximation between baryons and photons at all scales before decoupling; moreover we evolved perturbations in the massive neutrino component in a simplified way by switching off neutrinos perturbations when they were below the free streaming scale and treating them as a fluid above the free streaming scale.

-
- [1] See, e.g., D. Spergel et al., ApJS, 170, 377 (2007); M. Tegmark et al., Phys.Rev. D74 (2006) 123507; A. Riess et al., 2006, astro-ph/0611572
 - [2] M. Milgrom. ApJ, 207, 371 (1983); Jacob D. Bekenstein, Phys.Rev. D70 (2004) 083509
 - [3] G. Dvali, G. Gabadadze, M. Porrati. Phys.Lett. B485 (2000) 208; C. Deffayet, PLB, 502, 199 (2001);
 - [4] S. Carroll et al., Phys.Rev. D70 (2004) 043528; S. Carroll et al., Phys.Rev. D71 (2005) 063513;
 - [5] J. Uzan, F. Bernardeau. Phys.Rev. D64 (2001) 083004; M. White, C.S. Kochanek, 2001, ApJ, 560, 539; F. Bernardeau. arXiv:astro-ph/0409224; A. Shirata et al., Phys.Rev. D71 (2005) 064030; C. Sealfon, L. Verde & R. Jimenez, Phys.Rev. D71(2005) 083004; H. Stabenau, B. Jain, Phys.Rev. D74(2006)084007
 - [6] C. Skordis et al. Phys.Rev.Lett. 96 (2006) 011301; C. Skordis, Phys.Rev. D74 (2006) 103513
 - [7] S. Dodelson, M. Liguori. 2006, PRL 97 (2006) 231301
 - [8] A. Lue, R. Scoccimarro, G. Starkman. Phys.Rev. D69 (2004) 124015; L. Knox, Y.-S. Song, J.A. Tyson. 2005, astro-ph/0503644; M. Ishak, A. Upadhye, D. Spergel. Phys.Rev. D74 (2006) 043513
 - [9] K. Koyama, R. Maartens. JCAP 0601 (2006) 016
 - [10] T. Koivisto, H. Kurki-Suonio. Class.Quant.Grav. 23 (2006) 2355-2369; T. Koivisto. Phys.Rev. D73 (2006) 083517; B. Li, M.-C. Chu. Phys.Rev. D74 (2006) 104010;

- Y. Song, W. Hu, I. Sawicki. 2006, astro-ph/0610532; B. Li & J. Barrow. 2007, gr-qc/0701111
- [11] Pengjie Zhang. Phys.Rev. D73 (2006) 123504
 - [12] R. Bean et al., Phys.Rev. D75 (2007) 064020
 - [13] D. Huterer, E.Linder. 2006, astro-ph/0608681
 - [14] Jean-Philippe Uzan. 2006, arXiv:astro-ph/0605313.
 - [15] R. Caldwell, C. Cooray, A. Melchiorri, 2007, astro-ph/0703375
 - [16] L. Amendola, M. Kunz, D. Sapone, 2007, arXiv:0704.2421
 - [17] Roman Scoccimarro. Phys.Rev. D70 (2004) 083007
 - [18] M. Tegmark, A. Hamilton, Y. Xu. MNRAS, 335 (2002) 887
 - [19] P. Zhang & U.L. Pen 2005, PRL, 95, 241302
 - [20] J. Weller & A.M. Lewis, MNRAS, 346 (2003) 987; R. Bean & O. Dore, 2004, PRD, 69, 083503
 - [21] Martin Kunz, Domenico Sapone. 2006, astro-ph/0612452
 - [22] F. Bernardeau et al. Phys.Rept. 367 (2002) 1-248